Supplementary Figure 1. In silico evaluation of the *LMNB1* locus.

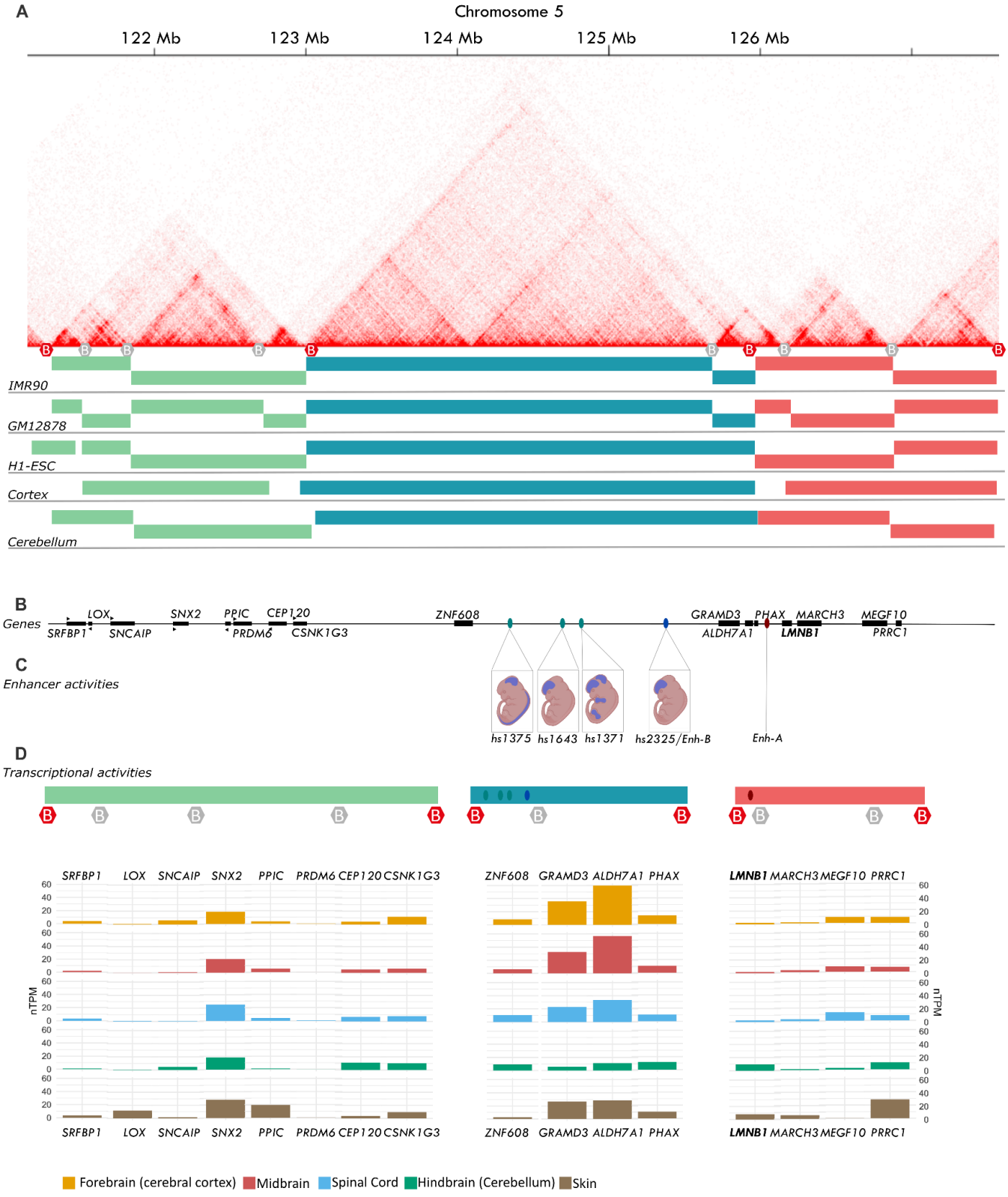

Supplementary Figure 1. In silico evaluation of the *LMNB1* locus.
(A) Hi-C heatmap derived from an in-house control shows the physiological TAD structure at the *LMNB1* locus (skin fibroblast; hg19; 10 kb resolution; raw count map). TADs (colored rectangles), boundaries ("B" within red hexagons) and anchor points ("B" within gray hexagons) at the locus for fibroblasts (IMR90), blood (GM12878), human embryonic stem cells (H1-ESC), cerebral cortex and cerebellum are shown (from the 3D Genome Browser). (B) Position of genes (black rectangles) and enhancers (colored ovals; from the VISTA Enhancer Browser) at the locus is reported. (C) The regulatory activities of VISTA enhancers in embryonic day 11.5 mouse embryos are represented in the diagrams (enhancer activities). Enh-A and Enh-B are already described in Giorgio et al., 2015. (D) A schematic representation of TADs, boundaries, anchor points and enhancers at the *LMNB1* locus is shown. Expression levels in the cerebral cortex, midbrain, spinal cord, cerebellum and skin of genes located within each TAD are reported as normalized transcript per million (nTPM; from Human Protein Atlas; RNA consensus tissue gene data).

Supplementary Figure 2. Hi-C heatmaps from further four ADLD patients.

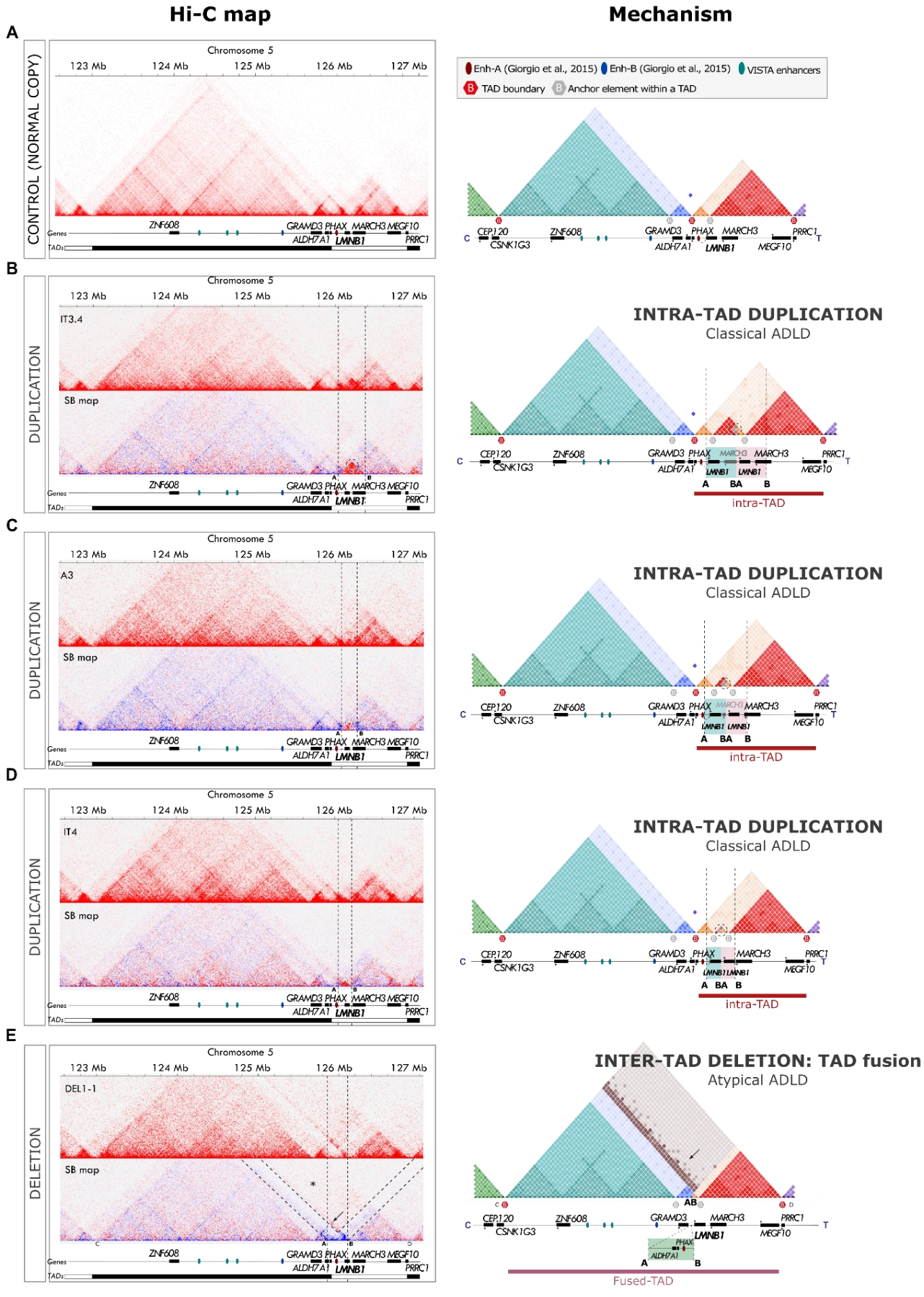

Supplementary Figure 2. Hi-C heatmaps from further four ADLD patients.
Hi-C heatmaps of the *LMNB1* locus and their graphical representations (right panels) are shown (skin fibroblast; hg19; 10 kb resolution; raw count map). For patients a second heatmap obtained with the subtraction method (SB map; patient - control) is reported. (A) Hi-C heatmap from a healthy subject shows the physiological TAD structure at the *LMNB1* locus (LMNB1 TAD in red; ALDH7A1, GRAMD3 and ZNF608 TAD in light blue; CEP120 TAD in green). (B-D) Hi-C and SB maps from patients IT3.4, A3 and IT4, carrying a *LMNB1* tandem duplication (highlighted with dot lines) of size 325 kb, 190 kb and 146 kb, respectively. The SB map emphasized the duplicated region as gain of interactions (red triangle) (in SB map, A and B pointed out the two breakpoints; dot circle shows the point of maximum interactions between A and B, corresponding to the new BA junction). On the right: the cartoon shows the linear representation of the allele carrying the duplication (the native and the extra *LMNB1* copies are highlighted in light blue and pink in the gene track below the respective map, respectively). The dot circles show the point of maximum interaction between A and B. All the SVs cause intra-TAD duplications. Notably, in all maps, *LMNB1* physiological regulatory element is never included in the duplication (E) Hi-C and SB map from DEL1-1 patient carrying a 250 kb deletion located upstream of the *LMNB1* gene (highlighted with dot lines). The SB map emphasized the deleted region as a V-shaped signature (dashed lines; A and B pointed out the two breakpoints). An overall increase in interactions between C and D is clearly stated (asterisk), suggesting a fused-TAD. The red stripe indicates the formation of new ectopic interactions between the *LMNB1* promoter and regulatory elements physiologically located in the adjacent TAD (arrow, enhancer adoption). On the right: the cartoon shows the linear representation of the allele carrying the deletion (in light green in the gene track below). The arrow points out the new ectopic interactions. The rearrangement causes the loss of a TAD boundary and the fusion of the two adjacent TADs (fused-TAD).

Supplementary Figure 3. Schematic overview of the inverted duplication.

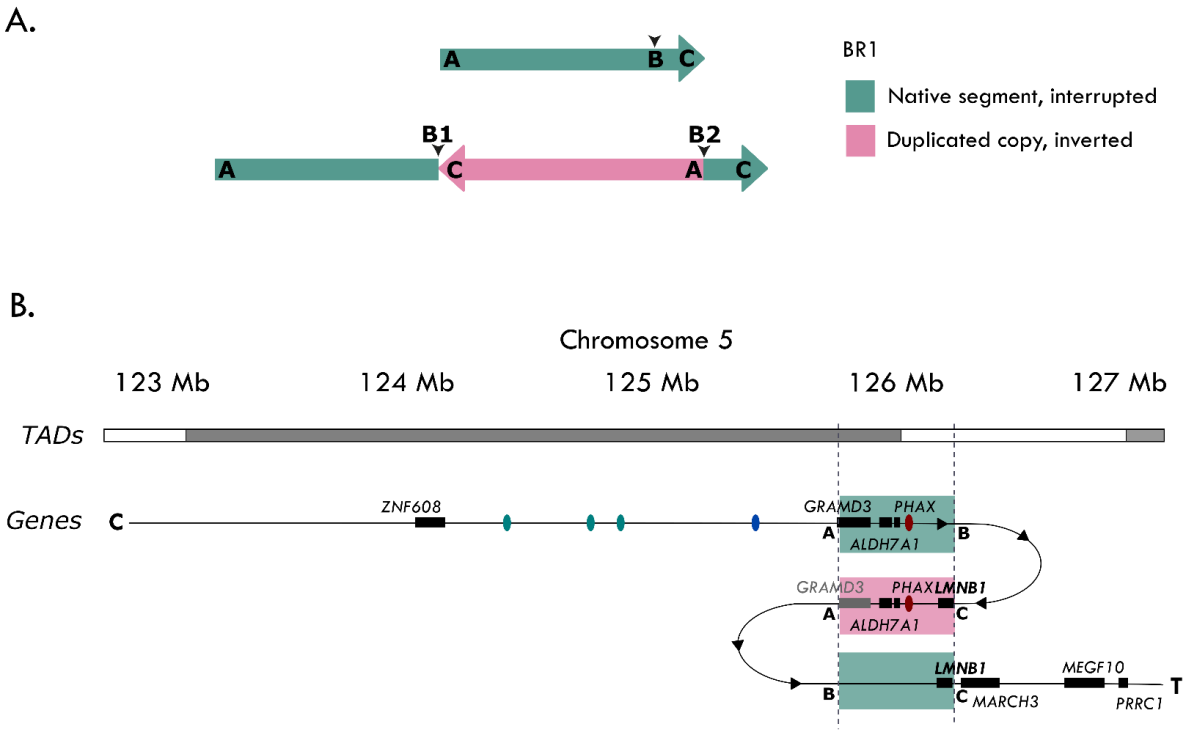

Supplementary Figure 3. Schematic overview of the inverted duplication.
Reconstruction of BR1 inverted duplication, adapted from Giorgio et al., 2013. (**A**) Schematic representation of the inverted duplication. The duplicated A-C segment is inverted and embedded between junctions B1 and B2. (**B**) Linear representation of BR1 inverted duplication in its genomic context, in relation to genes, TAD boundaries and regulatory elements located within the rearranged region. The native and duplicated segments are reported in teal green and pink, respectively. A-C breakpoints are highlighted by dashed lines.

Supplementary Figure 4. Presumed TAD structure alterations mediated by SVs not analyzed by Hi-C.

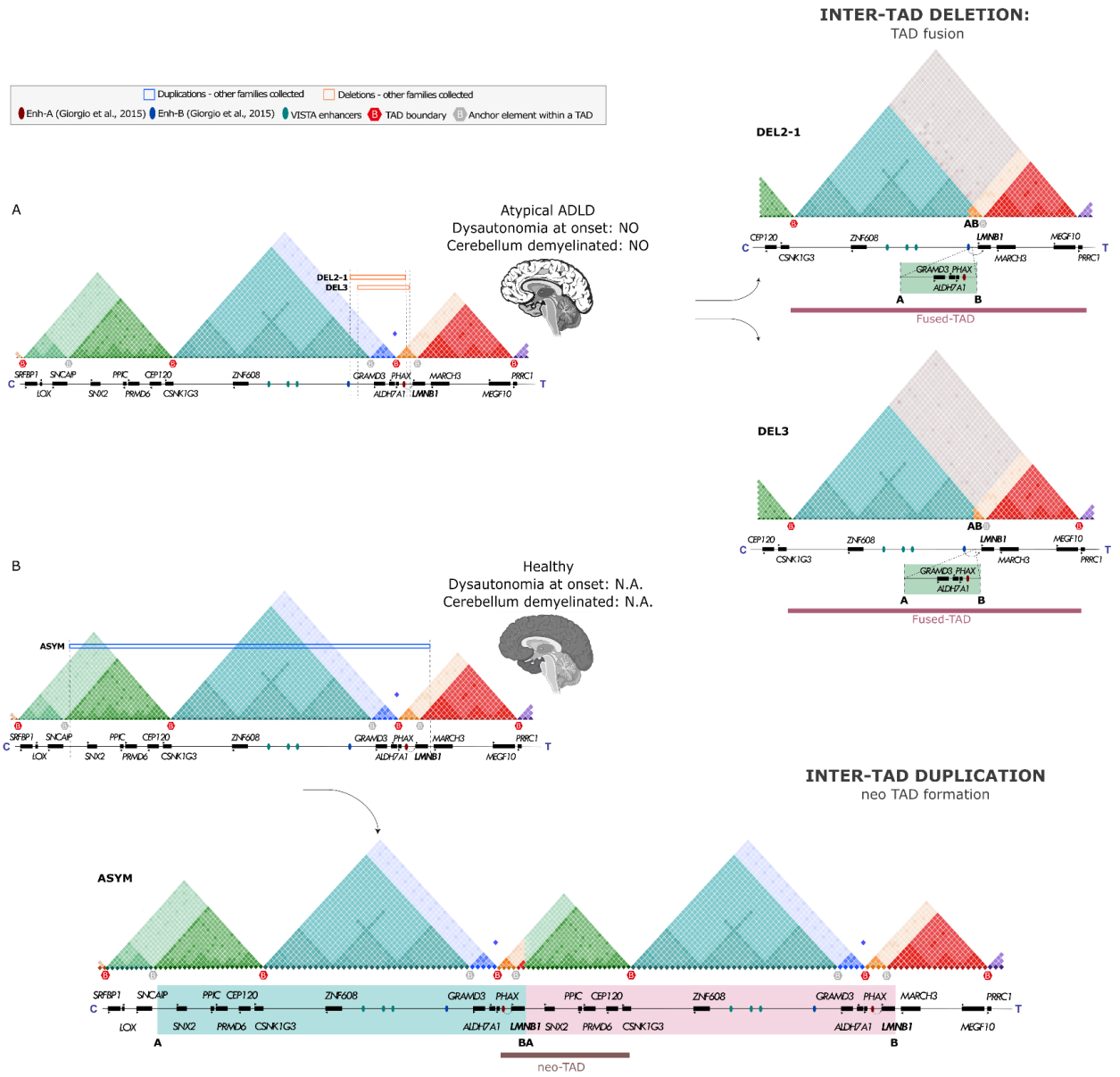

Supplementary Figure 4. Presumed TAD structure alterations mediated by SVs not analyzed by Hi-C. A schematic representation of the physiological TAD structure at the *LMNB1* locus (left), the associated clinical and neuroradiological phenotype (middle), and the proposed linear representation of the allele carrying the SV (right) is shown for each subject. On the left panel, the deleted/duplicated region is reported for each subject based on aCGH results (rectangles). (A) Patient DEL2-1 and DEL3 carrying a 672 and a 609 kb deletion upstream the *LMNB1* gene, respectively. On the right: cartoons showing the allele carrying the DEL2-1 and DEL3 deletions (reported in light green in the gene track below). The deletions are predicted to cause the loss of a TAD boundary and the fusion of the two adjacent TADs (Fused-TAD). Similar to ADLD-1-TO VI-1 (Fig.3C) and DEL1-1 (Suppl.Fig2E), the ectopic contacts within the fused-TAD are predicted to cause a comparable LMNB1 misexpression. (B) Asymptomatic subject (ASYM) carrying a 4.3 Mb tandem duplication encompassing the *LMNB1* gene and crossing three TADs and two boundaries (LMNB1 TAD in red; ALDH7A1, GRAMD3 and ZNF608 TAD in light blue; CEP120 TAD in green). On the right: the cartoon showing the allele carrying the duplication (the native and the extra *LMNB1* copies are highlighted in light blue and pink in the gene track below the map, respectively). The duplication is predicted to generate a neo-TAD containing the native *LMNB1* copy and its physiological regulatory element, and a regulatory region from the CEP120 TAD, likely preventing its expression in the brain of the carriers.

Supplementary Figure 5. Expression status of genes at the LMNB1 locus

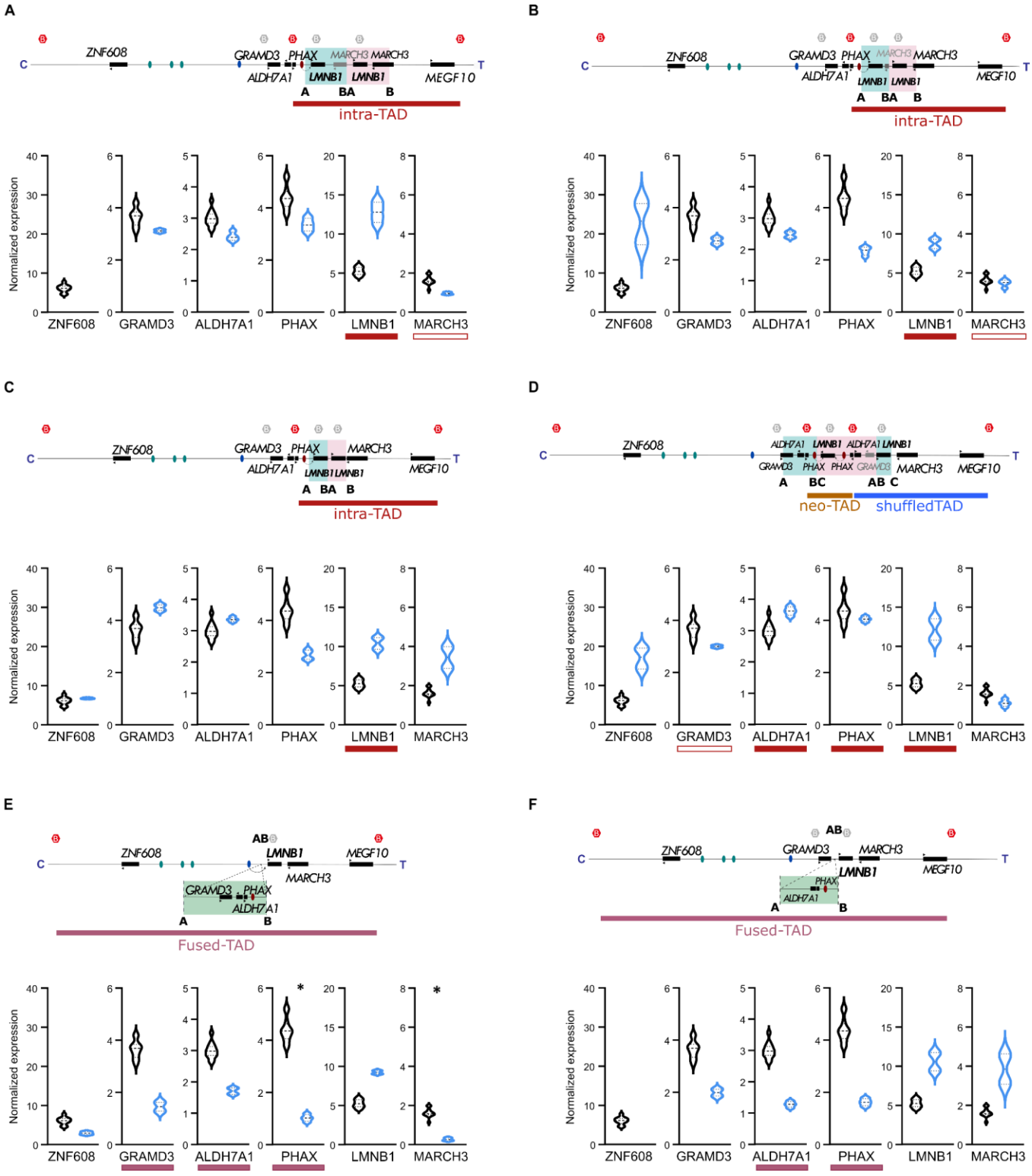

Supplementary Figure 5. Expression status of genes at the *LMNB1* locus. The cartoon shows the linear representation of the allele carrying the duplication (A-D) or the deletion (E-F). In duplicated carriers (A-D), the native and the extra *LMNB1* copies are highlighted in light blue and pink; in patients carrying a deletion upstream the gene (E-F), the deleted region is highlighted in light green (in the gene track below). TAD boundary and anchor points are represented as "B" within red or grey hexagons, respectively, whereas known enhancers regions are shown as colored ovals.
(**A-C**) Intra-TAD duplications encompass the *LMNB1* gene and a 3' region of the *MARCH3* gene in IT3 and A3 patients, whereas the SV includes exclusively the *LMNB1* gene in IT4 patient. Of note, *LMNB1* physiological regulatory element is never included in the duplication. (D) In BR1 patient the inverted duplication causes the formation of a neo-TAD with the extra copy of the *LMNB1* gene (in pink) and two copies of the *LMNB1* physiological element, and a shuffled-TAD with the native LMNB1 copy (in light blue) and regulatory elements from the adjacent TAD. Interestingly, due to the inversion, the shuffled TAD also includes two coding genes from the adjacent TAD, namely the *ALDH7A1* gene and a portion of the *GRAMD3* gene. (E-F) Inter-TAD deletions cause the loss of a TAD boundary and the fusion of the two adjacent TADs (fused-TAD). In ADLD-1-TO (E), the CNV includes three coding genes, namely *GRAMD3*, *ALDH7A1* and *PHAX*; whereas DEL1-1 deletion encompasses only *ALDH7A1* and *PHAX* genes. Patient-specific RNA-seq expression data are shown below each cartoon, the expression status of each gene [From DRAGEN Differential Expression tool (v4.2.4; Illumina), based on DESeq2 algorithm]. Black cloud: control; Light blue cloud: ADLD patient. Solid rectangles below gene names: fully duplicated/deleted genes; Void rectangles below gene names: partially duplicated/deleted genes; *: differentially expressed genes (adjusted p-value < 0.001; absolute log2 fold change > 2).

Supplementary Figure 6. Expression levels of genes at the *LMNB1* locus.

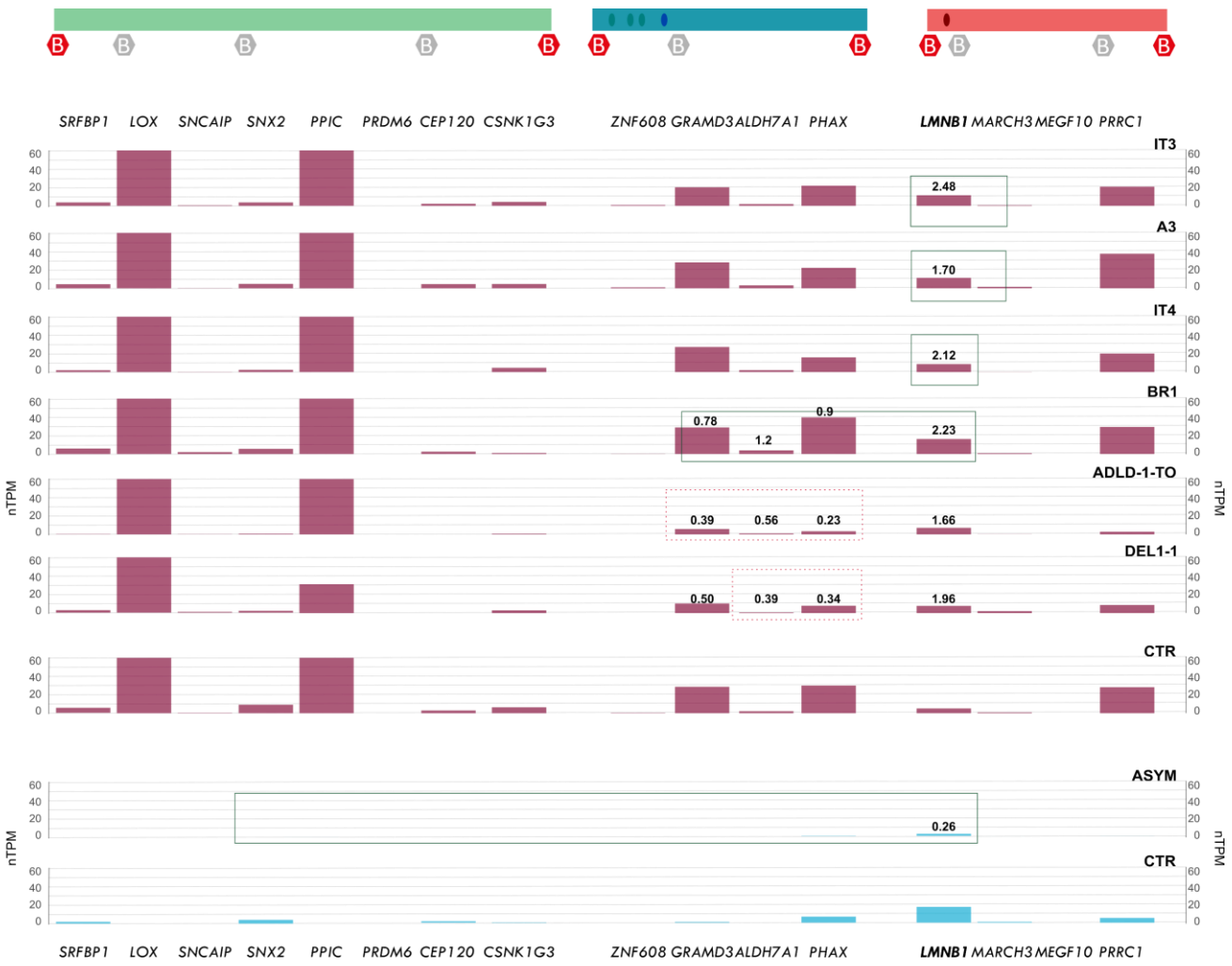

Supplementary Figure 6. Expression levels of genes at the *LMNB1* locus.
A schematic representation of TADs, boundaries, anchor points and enhancers at the *LMNB1* locus is shown. TAD boundary and anchor points are represented as "B" within red or grey hexagons, respectively, whereas known enhancers regions as colored ovals. Expression levels of genes located in the three TADs affected by SVs at the *LMNB1* locus is reported, as normalized transcript per million (nTPM). For each patient, genes involved in the SV are boxed (green rectangles: duplications; red dotted rectangles: deletions). For genes with an absolute log2 fold change > 0.75 [From DRAGEN Differential Expression tool (v4.2.4; Illumina)], the fold-change compared to the corresponding control is reported.

Supplementary Figure 7. CD68 and LMNB1 immunopositive cells.

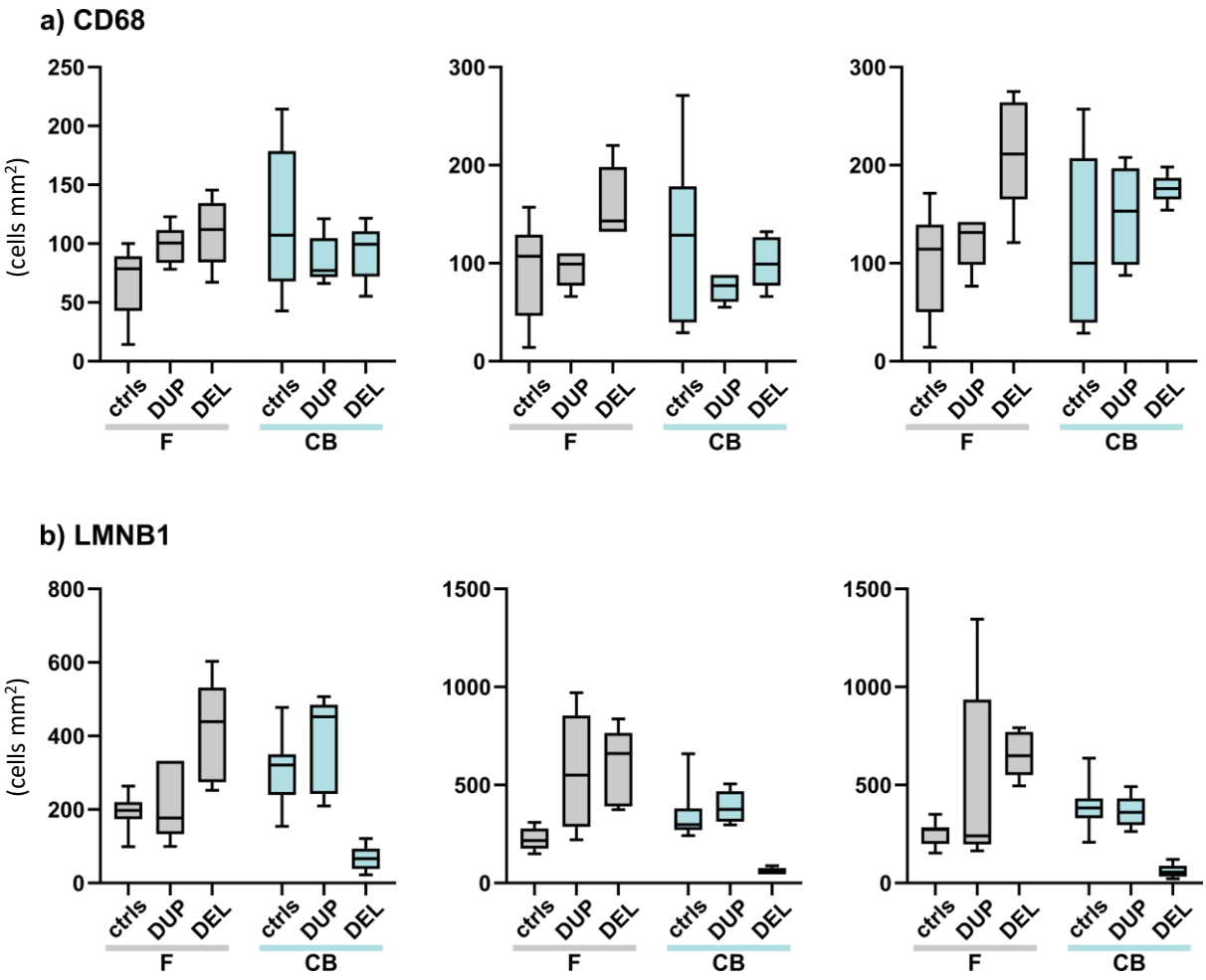

Supplementary Figure 7. CD68 and LMNB1 immunopositive cells.

Results of counting of CD68 (a) and LMNB1 (b) immunopositive cells in postmortem autopsy tissues from two controls (ctrls), a classical ADLD patient (555-10; DUP), and an atypical ADLD patient (ADLD-1-TO VI-7; DEL) are reported. Box and whiskers graphs represent cell count (cells per mm2) of five serial sections of autopsy tissue at 200× magnification for each specimen. Cell counting was blindly assessed by three experienced pathologists (left, middle and right panels). Controls: i) female, 35 years, legal euthanasia because of PTSS; ii) female, 24 years, myocarditis. Cerebrum: frontal white matter (F); Cerebellum: cerebellar white matter (CB).